A Fundamental Study on Damping Control Design using PMU signals from Dominant Inter-Area Oscillation Paths

Yuwa Chompoobutrgool *Student Member, IEEE*, and Luigi Vanfretti, *Member, IEEE*.

***Abstract*—This article presents a fundamental study on feedback control using different types of signals available from a dominant inter-area oscillation path; the passageway containing the highest content of the inter-area oscillations. Results from the previous studies verify the persistence and robustness of dominant path signals and suggest that using such signals, effective damping control may be achieved. To corroborate the implication, signals available from phasor measurement units (PMU) e.g. voltage phasors (magnitude and angle) from the dominant path are used as feedback inputs for a power system stabilizer (PSS) control design for damping enhancement. The corresponding performance are compared with those using generator speed, which is a commonly used signal though not available from PMUs, as inputs. Contrary to expectations found in common practice, that of speed being the one of the most effective signal for damping control, it is demonstrated here that their corresponding damping performance is inferior to those using voltage phasors as feedback inputs. A conceptualized two-area system is used to analyze damping performance throughout this study.**

***Index Terms*—feedback input signals selection; network modeshapes; dominant paths; PMU.**

I. Introduction

One major challenge in damping control design is the selection of feedback input signals. Conventionally, power system stabilizers (PSSs) use local measurements as input signals such as active power in the outgoing transmission line, generator speed, and frequency at the terminal bus. With the availability of signals from phasor measurement units (PMUs), choices of inputs are not only limited to those local but now include wide-area signals. Several studies suggest that wide-area signals are preferable to local signals [1], [2]. Therefore, the exploitation of PMU signals is desirable. However, the main issue is which signal, among all the available signals, would give satisfactory damping performance.

The concept of "interaction paths" was used to characterize the dynamic behavior of the Western Electric Coordinating Council (WECC) power system in [3], where the interaction paths are defined as the group of transmission lines, buses, and controllers which the generators in a system use for exchanging energy during swings. Building upon this notion, we have established the concept "dominant inter-area oscillation paths" which are defined as the passageways containing the highest content of the inter-area oscillations. The persistence of the paths and the robustness of the signals on the paths are justified in the previous studies [4], [5] where the results suggest that effective damping control can be achieved by using signals from the dominant paths.

The aim of this article is thus to carry out a fundamental study on feedback control using PMU signals from a dominant path. As such, a conceptualized two-area system is used to illustrate PSS control design for damping enhancement. Three types of signals, namely voltage magnitude, voltage angle, and generator rotor speed, are used as inputs for a PSS controller. The first two types represent the signals available from PMU while the latter represents one of the most commonly used signal in PSS damping design. Their corresponding performances are analyzed and compared. The results of this study offer promising and feasible choices of signals to be used in feedback control. Although only PSS is considered, the concepts are applicable for any other damping controllers.

II. Basis of Study

A. Network Modeshape (S)

The concept of dominant paths can be quantitatively expressed by the product of the two key factors: mode shapes belonging to electromechanical oscillations and sensitivities of network variables. This relationship is termed "network modeshape" [6], [7]. It indicates how much of the content of each mode is distributed within the network variables. In other words, the larger in magnitude the network modeshape is, the more observable the signals measured from the path become. The variables of interest are voltage magnitude and voltage angles since they are directly measured by the PMUs. Thus, only their corresponding modeshapes, S_V and S_θ, are considered in this study.

Consider a linearized N-machine system in a state-space form

$$\Delta\dot{x} = A\Delta x + B\Delta u, \quad \Delta y = C\Delta x + D\Delta u, \tag{1}$$

where vectors Δx, Δy, and Δu represent the state variables, the output variables and the inputs, respectively. With no input, the electromechanical model is expressed as

$$\underbrace{\begin{bmatrix}\Delta\dot{\delta}\\ \Delta\dot{\omega}\end{bmatrix}}_{\Delta\dot{x}} = \underbrace{\begin{bmatrix}A_{11} & A_{12}\\ A_{21} & A_{22}\end{bmatrix}}_{A}\underbrace{\begin{bmatrix}\Delta\delta\\ \Delta\omega\end{bmatrix}}_{\Delta x} \tag{2}$$

where matrix A represent the state matrix corresponding to the state variables $\Delta\delta$ and $\Delta\omega$. Then, performing eigenanalysis, the electromechanical mode shape is derived from

$$AW(A) = \lambda W(A) \tag{3}$$

where λ are eigenvalues of the electromechanical modes of the system and $W(A)$ are the right eigenvectors or mode shape that is used to compute the network modeshape.

The authors are with KTH Royal Institute of Technology, Stockholm, Sweden. E-mail: yuwa@kth.se, luigiv@kth.se

Y. Chompoobutrgool is supported by Elforsk, Sweden.

L. Vanfretti is supported by the STandUP *for* Energy collaboration initiative, Nordic Energy Research through the STRONg^2*rid* project and the European Commission through the *i*Tesla FP7 project.

978-1-4673-2308-6/12/$31.00 ©2012 IEEE

Using C from (1), sensitivities of the voltage magnitude (C_V) and voltage angle (C_θ) are expressed as

$$\underbrace{\begin{bmatrix}\Delta V\\ \Delta\theta\end{bmatrix}}_{\Delta y} = \underbrace{\begin{bmatrix}\frac{\partial V}{\partial\delta} & \frac{\partial V}{\partial\omega}\\ \frac{\partial\theta}{\partial\delta} & \frac{\partial\theta}{\partial\omega}\end{bmatrix}}_{C}\underbrace{\begin{bmatrix}\Delta\delta\\ \Delta\omega\end{bmatrix}}_{\Delta x} = [C_V \quad C_\theta]^T\begin{bmatrix}\Delta\delta\\ \Delta\omega\end{bmatrix} \tag{4}$$

Then, the expressions for voltage magnitude and voltage angle modeshapes (S_V and S_θ) are

$$S_V = C_V W(A), \quad S_\theta = C_\theta W(A). \tag{5}$$

B. Conceptualization of the Dominant Inter-Area Paths

Consider a conceptualized two-area system shown in Fig. 1, G_1 and G_2 represent the main clusters of machines involved in the inter-area swing while transformers and line impedances represent elements of the dominant path connecting the two areas.

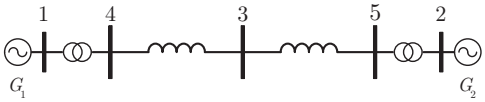

Fig. 1. Conceptualization of a two-area, two-machine system.

This conceptual system is modelled as follows. Generator 1 (G_1) is represented by a sixth-order machine model and a static excitation system model whereas Generator 2 (G_2) is represented by a third-order machine model. The power transfer from G_1 to G_2 is 1100 MW. The inter-area mode of the system is $-0.0162 \pm j2.3485$, which has a frequency and damping ratio of 0.3738 Hz and 0.6908%, respectively.

Characteristics of the dominant inter-area paths[1] can be demonstrated using the computed voltage magnitude (S_V) and angle modeshapes (S_θ) as illustrated in Fig. 2. The x-axis represents the bus number in the dominant path; the distance between buses are proportional to the line impedance magnitude. According to the figure, important features of the dominant path are summarized below.

- The largest S_V or the smallest S_θ element(s) indicates the center of the path. This center can be theorized as the "inter-area mode center of inertia" or the "inter-area pivot" for each of the system's inter-area modes.
- The difference between S_θ elements of two edges of the path are the largest among any other pair within the same path. In other words, the oscillations are the most positive at one end while being the most negative at the other end. Hence, they can be theorized as the "tails" for each inter-area mode.
- S_V elements of the edges are the smallest or one of the smallest within the path.

III. Damping Controller Design

A. Controller Structure

The objective of the design is to improve damping of the inter-area mode by installing a PSS at G_1 modulating the AVR

[1]These are similar to the characteristics of voltage change and angle change of the first swing mode in Fig.13 [8] where the mode is described by a single wave equation with one spatial dimension.

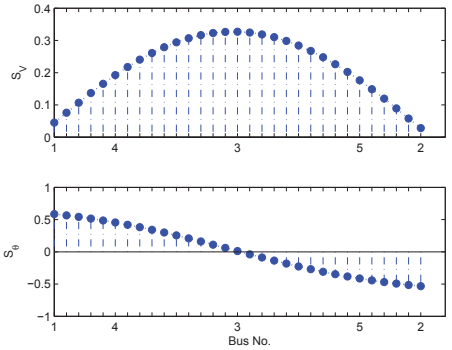

Fig. 2. Voltage magnitude and angle modeshapes of the dominant path in the two-area system.

error signal. Following the design in [9], the structure of the PSS includes lead/lag compensators in the form

$$PSS = K_d\left[\alpha\frac{s+z}{s+p}\right]^n\frac{T_w s}{1+T_w s} \tag{6}$$

where n is the number of compensator stages and T_w is the washout filter having the value of 10 s. Note that generator speed, as well as angle difference, has high components of torsional modes [10]. Therefore, a torsional filter is added to the PSS structure when generator speed and angle differences are used as feedback input signals. The torsional filter used has the form

$$G_{tor}(s) = \frac{1}{0.0027s^2 + 0.0762s + 1}. \tag{7}$$

α, poles (p), and zeros (z) can be computed from the following equations:

$$\phi_m = \frac{180^\circ - \theta_{dep}}{n}, \alpha = \frac{1+sin(\phi_m)}{1-sin(\phi_m)}, p = \sqrt{\alpha}\omega_c, p = \alpha z \tag{8}$$

where $\theta_{dep}, \phi_m,$ and ω_c represent angle of departure of the inter-area mode, angle compensation required, and the frequency of the mode in rad/sec.

B. Feedback Input Signals

In this study, the impact of different feedback input signals on the damping of the two-area test system will be evaluated. Each signal requires different controller (PSS) parameters, as well as different structures. As such, two analyses are carried out to assess damping performance. They are

1) Controller design for maximum damping, and
2) controller design using fixed-structure controllers.

In the first analysis, for each input signal, PSS parameters will be tuned such that the system achieves its highest damping possible. The second analysis considers practical issues; PSS parameters and structures are generally fixed. Therefore, corresponding system performance (using different signals) should be evaluated.

For each analysis, voltage magnitude, voltage angle, and generator speeds will be used as feedback input signals. Controller performance is evaluated considering the following factors: (1) distance from zeros close to the inter-area mode (d_λ) (it is desirable for the zeros to be far from the inter-area mode [11]), (2) effective gain (the cumulative gain of the PSSs

which can be computed from $\alpha^n K_d$), (3) damping ratio (ξ), (4) overshoot (M_p), and (5) rise time (t_r.)

The monitored signal is the bus voltage terminal at G_1, V_1, whereby its response is evaluated by the above factors.

C. Controller Design Illustration

In this illustration, signal V_3, the voltage magnitude at Bus 3, is used as the feedback input signal. A root-locus plot of the open-loop system (no phase compensation) including the washout filter is shown in Fig. 3a. The angle of departure (θ_{dep}) of the inter-area mode is $-23.03°$. Using this angle, PSS parameters are computed using equations (6-8). Adding the designed controller to the system, the root-locus plot is shown in Fig. 3b which shows an inverse direction of the inter-area mode; i.e., the inter-area mode is moving in a stable direction. Gain K_d is obtained when moving along the branch of the root loci of the inter-area mode until the desired damping ratio, or maximum damping in this case, is reached. Finally, for the signal used, the obtained PSS has the form

$$PSS = 0.00372 \left[98 \frac{s + 0.2372}{s + 23.249}\right]^2. \quad (9)$$

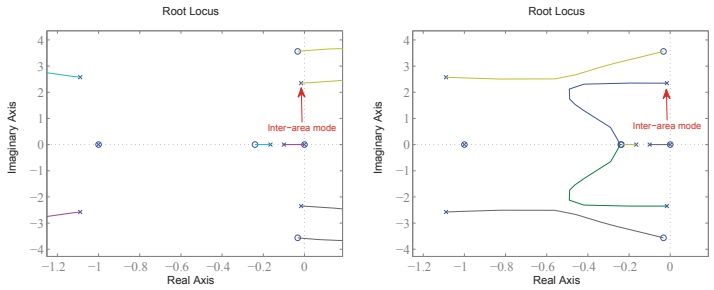

(a) No phase compensation. (b) With phase-lead compensation.

Fig. 3. Root-locus plots of the system with V_3 as feedback input signal.

Responses of the terminal voltage at Bus 1 with and without PSS are compared in Fig. 4.

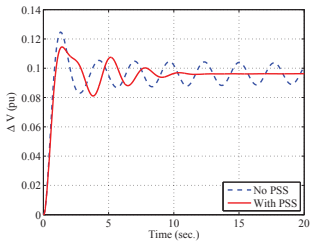

Fig. 4. Damping control performance using V_3 as feedback input signal.

This design process will be repeated using different input signals in the following sections.

IV. Controller Design for Maximum Damping

A. Voltage Magnitude

The system's damping performance using voltage magnitudes as feedback input signals is summarized in Table I. Note that they are arranged in the order of the dominant path in Fig. 1. All voltage magnitude signals use 3-stage lead compensator.

TABLE I
System Performance using Voltage Magnitudes as Feedback Input Signals.

Signals	d_λ	Effective gain	ξ (%)	M_p (%)	t_r (s)
V_1	0.09	53.55	2.73	-	2.35
V_4	0.44	48.44	7.41	14.79	0.83
V_3	1.21	35.73	22.5	14.54	0.64
V_5	1.97	123.72	20.2	17.77	0.69
V_2	»	478.43	6.83	15.82	0.61

Note: Controller with maximum damping.

TABLE II
System Performance using Combination of Voltage Magnitude as Feedback Input Signals.

Signals	d_λ	Effective gain	ξ (%)	M_p (%)	t_r (s)
V_4	0.44	48.44	7.41	14.79	0.83
$V_3 + V_4$	0.73	15.11	12.95	18.1	0.65
$V_4 + V_5$	0.69	22.11	12.3	17.41	0.66
$V_3 + V_4 + V_5$	0.87	13.15	14.86	16.54	0.65

Note: Controller with maximum damping.

According to the results in Table I, it can be concluded that damping performance, together with effective gain, correspond to the voltage magnitude modeshape (S_V) (see Fig. 2) where V_3 having the largest S_V achieves the highest damping performance and requires the least amount of gain.

Table I's corresponding responses of the terminal voltage at Bus 1 are illustrated in Fig. 5a.

Sets of possible signal combinations using voltage magnitude are shown in Table II. Here, different combinations of Bus 4 with Bus 3 and Bus 5 are investigated. Note that "»" in the distance column indicates that the distance is much larger than 100.

Comparing to only using a single signal (V_4), using signal combination improves the damping of the system. Furthermore, the effective gain is considerably reduced, to more than half, as a result of combining signals. Comparing the sets $V_3 + V_4$ to $V_3 + V_4 + V_5$, both combinations require relatively about the same gain, however, the latter achieves higher damping. On the other hand, if this combined signals ($V_3+V_4+V_5$) were to be implemented, when one of the signals is lost and the controller parameters are fixed for the combined signal, the resulting damping will decrease, as shown in the forthcoming analysis.

Table II's corresponding responses of the terminal voltage at Bus 1 are illustrated in Fig. 6a.

B. Angle Differences

The system performance using voltage angle differences as feedback input signals is summarized in Table III. All angle differences in Table III use a 1-stage lag compensator. Note that θ_4 is used as a reference and $\Delta\theta_{ij}$ represents the difference between two angles: $\theta_i - \theta_j$.

According to the results in Table III, it can be concluded that both damping performance and effective gain correspond to the voltage angle modeshape (S_θ) in which $\Delta\theta_{24}$ having the largest S_θ achieves the highest damping ratio with smallest gain.

Table III's corresponding responses of the terminal voltage at Bus 1 are illustrated in Fig. 7a. Note that, in order to have

TABLE III
SYSTEM PERFORMANCE USING ANGLE DIFFERENCES AS FEEDBACK INPUT SIGNALS.

Signals	d_λ	Effective gain	ξ (%)	M_p (%)	t_r (s)
$\Delta\theta_{41}$	1.54	0.86	14.2	71.1	0.54
$\Delta\theta_{34}$	2.357	0.21	16.63	40.89	0.55
$\Delta\theta_{54}$	2.359	0.12	17.74	40.28	0.56
$\Delta\theta_{24}$	2.360	0.09	18.85	30.94	0.56

Note: Controller with maximum damping.

TABLE IV
SYSTEM PERFORMANCE USING ANGLE DIFFERENCES AS FEEDBACK INPUT SIGNALS: TWO-AREA CASE.

Signals	d_λ	Effective gain	ξ (%)	M_p (%)	t_r (s)
$\Delta\theta_{12}$	42.08	85.37	20.32	21.04	0.61
$\Delta\theta_{avg,1}$	33.82	44.87	20.00	19.25	0.61
$\Delta\theta_{avg,2}$	26.12	91.40	21.24	27.82	0.63

Note: Controller with maximum damping.

the same sign, $\Delta\theta_{41}$ is used instead of $\Delta\theta_{14}$.

Sets of possible signal combinations using angle differences between the two areas are shown in Table IV where the average angle differences $\Delta\theta_{avg,1}$ represents $(\theta_1+\theta_4)-(\theta_2+\theta_5)$ and $\Delta\theta_{avg,2}$ represents $(\theta_a+\theta_4)-(\theta_b+\theta_5)$. Note that Bus a is a bus in the middle between Bus 4 and Bus 3, whereas Bus b is a bus in the middle between Bus 3 and Bus 5. The aim of using the average angle differences in the two areas is to reduce the effect of the local oscillations [11]. All two-area angle difference combinations use a 2-stage lead compensator.

By combining signals from both areas, the damping performance does not increase significantly but the overshoot is greatly reduced, as compared to those in Table III. For example, the overshoot of $\Delta\theta_{24}$ is larger those that of $\Delta\theta_{avg,1}$ and $\Delta\theta_{avg,2}$ while the damping ratio improves about 1-2 % when using the averaged signals. However, the effective gain increases as a result of using two-area combinations. In practice, θ_1 and θ_2 are generator buses and thus not usually available from PMUs (see [12]). Hence, for any practical implementation, the most feasible combination is $\Delta\theta_{avg,2}$, for which similar damping performance can be achieved, although, notice that, a higher gain is the price to pay.

Table IV's corresponding responses of the terminal voltage at Bus 1 are illustrated in Fig. 8a.

C. Generator Speed

For comparison purposes, we consider speed signals from generators-although, only available locally, and not available from PMUs [12]. The system performance using generator speed as feedback input signals is summarized in Table V. All signals in Table V use a 2-stage lead compensator except for ω_2 which requires a 3-stage lead compensator.

According to the results in Table V, overall, using speed as feedback input signals requires considerably larger gain than using other signals, especially using ω_2.

Contrary to expectations founded in common practice, that of speed being one of the most effective signal for damping control, it is demonstrated here that using $\Delta\theta_{ij}$ as input signals, higher damping performance can be obtained while using much lower effective gain. The maximum damping obtained from speed signals is lower than the maximum

TABLE V
SYSTEM PERFORMANCE USING GENERATOR SPEED AS FEEDBACK INPUT SIGNALS.

Signals	d_λ	Effective gain	ξ (%)	M_p (%)	t_r (s)
ω_1	»	349.19	16.89	27.2	0.63
ω_2	2.35	266632.35	15.4	32.49	0.47
$\omega_1-\omega_2$	»	227.38	16.06	31.31	0.66
$0.5*(\omega_1-\omega_2)$	»	287.68	16.7	22.25	0.61

Note: Controller with maximum damping.

TABLE VI
SYSTEM PERFORMANCE USING VOLTAGE MAGNITUDE AS FEEDBACK INPUT SIGNALS.

Signals	ξ (%)	M_p (%)	t_r (s)
V_1	2.41	25.63	0.67
V_4	9.05	20.37	0.67
V_3	22.5	14.54	0.64
V_5	9.6	18.18	0.59
V_2	1.55	23.39	0.56

Note: Controller with fixed parameters.

damping that can be obtained from $\Delta\theta_{ij}$. Compare $\Delta\theta_{12}$ to $\omega_1-\omega_2$, the angle difference outperforms the speed signals in damping performance, effective gain required and overshoot[2].

Table V's corresponding responses of the terminal voltage at Bus 1 are illustrated in Fig. 9a.

V. DESIGN FOR FIXED PARAMETER PSSS

A. Voltage Magnitude

The system damping performance using voltage magnitudes as feedback input signals with a fixed controller (both parameters and structure) is summarized in Table VI. The PSS parameters are $\alpha=98, K_d=0.00372$ using a 2-stage lead compensator. The resulting effective gain is 35.73.

The results in Table VI correspond to the voltage magnitude modeshape, S_V, where V_3 having the largest S_V is the most effective signal (highest damping performance). An important observation is that for a controller designed to use a specific signal, a lower damping should be expected if the original signal is replaced by another. In addition, there might be some side effects due to inadequate phase compensation.

Table VI's corresponding responses of the terminal voltage at Bus 1 are illustrated in Fig. 5b.

For the signal combination scenario, a different structure of controller is used: $\alpha=93, K_d=0.00152$ using a 2-stage lead compensator. The resulting effective gain is 13.15.

If the last combination $V_3+V_4+V_5$ with highest damping were to be implemented as input to the PSS, when one of the signals is lost, this results in damping reduction.

Table VII's corresponding responses of the terminal voltage at Bus 1 are illustrated in Fig. 6b.

B. Angle Differences

The system performance using voltage angle differences as feedback input signals with fixed controller is summarized in Table VIII. The PSS parameters are $\alpha=1.4856, K_d=0.0578$

[2]Although, it is noted that none of the signals are actually available from PMUs: $\Delta\theta_{12}$ due to placement practice [12] and $\omega_1-\omega_2$ due to PMU characteristics [11]

TABLE VII
SYSTEM PERFORMANCE USING COMBINATION OF VOLTAGE MAGNITUDE AS FEEDBACK INPUT SIGNALS.

Signals	ξ (%)	M_p (%)	t_r (s)
$V_3 + V_4$	11.23	18.75	0.63
$V_4 + V_5$	7.39	20.24	0.62
$V_3 + V_4 + V_5$	14.86	16.54	0.65

Note: Controller with fixed parameters.

TABLE VIII
SYSTEM PERFORMANCE USING ANGLE DIFFERENCE AS FEEDBACK INPUT SIGNALS.

Signals	ξ (%)	M_p (%)	t_r (s)
$\Delta\theta_{41}$	-0.77	23.81	0.56
$\Delta\theta_{34}$	6.57	28.92	0.56
$\Delta\theta_{54}$	15.00	31.12	0.56
$\Delta\theta_{24}$	18.85	30.94	0.56

Note: Controller with fixed parameters.

using a 1-stage lag compensator. The resulting effective gain is 0.09.

As can be expected from the angle modeshape, S_θ, result, the combination $\Delta\theta_{24}$ having the largest angle difference modeshape achieves the highest damping performance. As previously stated, θ_2 is not likely to be available from PMUs and, thus, if θ_5 is to replace it, the resulting damping is lower than using θ_2.

Table VIII's corresponding responses of the terminal voltage at Bus 1 are illustrated in Fig. 7b. The responses of $\Delta\theta_{41}$ highlights the fact that controller structure and parameters need to change depending on the input signals. Note that from Table VIII when $\Delta\theta_{41}$ is used with the controller designed for $\Delta\theta_{24}$, this results in negative damping, rendering the system unstable.

Sets of possible signal combinations using angle differences between the two areas with fixed controller are shown in Table IX. The PSS parameters are $\alpha = 418.05, K_d = 0.000523$ using a 2-stage lead compensator. The resulting effective gain is 91.4.

The results show that using the same amount of gain, similar damping can be obtained when using the angle difference or the average values between the two areas.

Table IX's corresponding responses of the terminal voltage at Bus 1 are illustrated in Fig. 8b.

C. Generator Speed

The system performance using generator speed as feedback input signals with a fixed controller is summarized in Table X. The PSS parameters are $\alpha = 5.66, K_d = 10.9$ using a 2-stage lead compensator. The resulting effective gain is 349.19.

With a fixed controller, using the signal ω_2 as the feedback

TABLE IX
SYSTEM PERFORMANCE USING ANGLE DIFFERENCE AS FEEDBACK INPUT SIGNALS: TWO-AREA CASE.

Signals	ξ (%)	M_p (%)	t_r (s)
$\Delta\theta_{12}$	14.07	16.79	0.57
$\Delta\theta_{avg,1}$	20.55	11.11	0.59
$\Delta\theta_{avg,2}$	21.24	27.82	0.63

Note: Controller with fixed parameters.

TABLE X
SYSTEM PERFORMANCE USING GENERATOR SPEED AS FEEDBACK INPUT SIGNALS.

Signals	ξ (%)	M_p (%)	t_r (s)
ω_1	16.89	27.2	0.63
ω_2	-19.25	»100	0.52
$\omega_1 - \omega_2$	18.64	44.27	1.36
$0.5 * (\omega_1 - \omega_2)$	16.83	26.64	0.63

Note: Controller with fixed parameters.

input signal results in instability; damping is negative[3]. This emphasizes the necessity and importance of choosing the "appropriate" signals as feedback inputs.

Table X's corresponding responses of the terminal voltage at Bus 1 are illustrated in Fig. 9b.

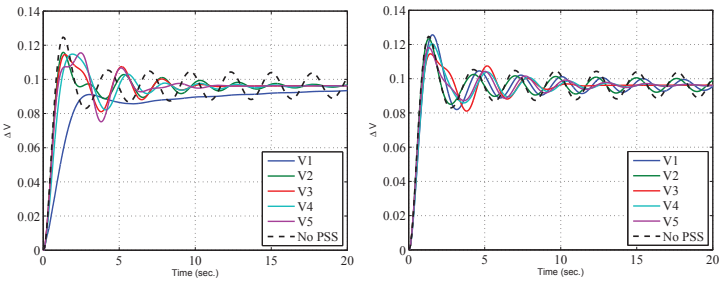

(a) Maximum damping. (b) Fixed PSS.

Fig. 5. Damping control performance using V_i as feedback input signals.

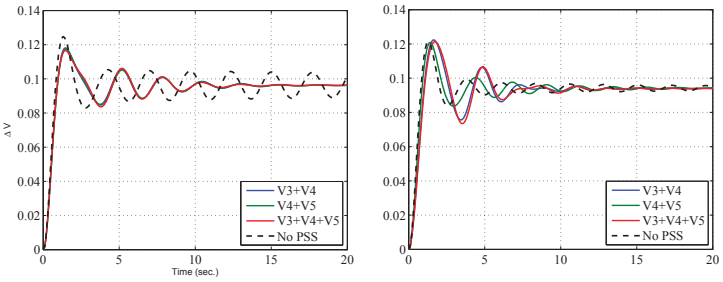

(a) Maximum damping. (b) Fixed PSS.

Fig. 6. Damping control performance using $\sum V_i$ as feedback input signals.

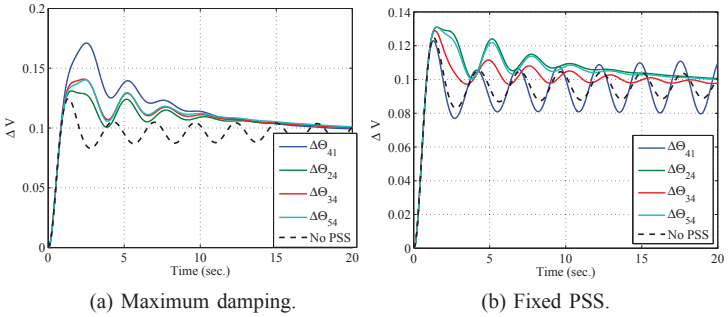

(a) Maximum damping. (b) Fixed PSS.

Fig. 7. Damping control performance using $\Delta\theta_{ij}$ as feedback input signals.

VI. CONCLUSION

Results from both analyses indicate that angle difference is the most effective feedback input signals with comparatively

[3]For this signal to be effective, proper manipulations or phase compensation would be needed.

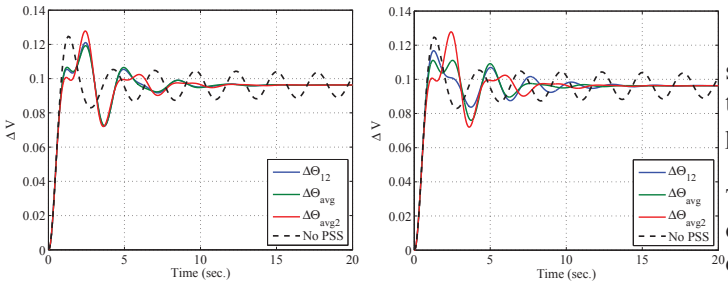

(a) Maximum damping. (b) Fixed PSS.

Fig. 8. Damping control performance using two-area $\Delta\theta_{ij}$ as feedback input signals.

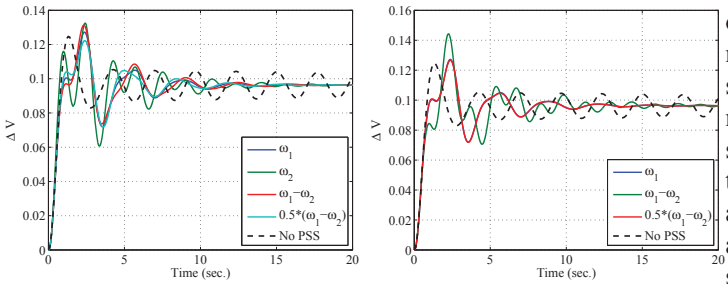

(a) Maximum damping. (b) Fixed PSS.

Fig. 9. Damping control performance using two-area ω_i as feedback input signals.

superior damping performance and small effective gain required, comparing to voltage magnitude and generator speed. Although one drawback of using angle difference is large overshoot, which can be reduced by combining and averaging signals from two areas.

Damping performance of each signal of the voltage magnitude and angle differences is in accordance with their corresponding network modeshapes (see Fig. 2). That is, signals having high network modeshape achieve higher damping ratios than those with lower network modeshaps.

In the second analysis where the PSS parameters are fixed (as it is today's practice), it can be concluded that by using different types of inputs, one cannot always expect to attain sufficiently high damping; this depends on the resulting location of the zeros near the inter-area mode. Closed-loop observability of inter-area modes will be different than open-loop observability due to the effect of "d_λ": the distance of the zeros of an open-loop system closest to the inter-area mode.

In the case of voltage magnitude, when a signal with a small d_λ, e.g. V_4 with $d_{\lambda 4} = 0.44$, is combined with a larger d_λ-signal, e.g. V_5 with $d_{\lambda 5} = 1.97$, the combination results in $d_{\lambda 45} = 0.69$ which is larger than that of $d_{\lambda 4}$ but smaller than $d_{\lambda 5}$. Note that, in practice, if PMUs are available at Bus 4 and Bus 5 and Bus 4 is used as a primary signal, complementing V_4 with V_3 and V_5 provides damping enhancement because the distance to zero increases. However, when V_5 is a primary signal for damping, V_4 should be used only as a backup.

Observe that when combining a signal with a short d_λ, e.g. $d_{\lambda 4}$ with two signals with larger d_λ, e.g. $d_{\lambda 3}$ and $d_{\lambda 5}$, the resulting d_λ will increase the damping.

In contrast to the common practice that often use generator speed as feedback inputs, the speed signals are not proven to be the best option (not to mention that the signals are not practically available from PMUs).

Different loading effects are not yet considered in this study. This is relevant because, for different loading scenarios, the open-loop observability of the dominant path signals shifts depending on loading level. Further work is necessary to determine if the closed-loop observability on different loading levels maintains the same properties as revealed in this study.

The selection of the "right" input signals from PMUs is critical for effective damping control. However, in the case of signal loss (due to communication failures), the controller must be changed even if new signals are to replace a lost signal so that highest damping can be obtained. These changes must occur adaptively and must be initiated by an adequate switch-over logic that guarantees the continued operation of the damping controller. Depending on the types of signals as well as signal combination, controller structure must be adapted accordingly to achieve optimal damping possible. As such, "adaptive" controllers, which can automatically adjust their parameters for each input signal feeding in, are promising and desirable.

REFERENCES

[1] M. Aboul-Ela, A. Sallam, J. McCalley, and A. Fouad, "Damping Controller Design for Power System Oscillations using Global Signals," *IEEE Transactions on Power System*, vol. 11, no. 2, pp. 767–773, May 1996.

[2] J. Chow, J. Sanchez-Gasca, H. Ren, and S. Wang, "Power System Damping Controller Design Using Multiple Input Signals," *IEEE Control System Magazine*, pp. 82–90, August 2000.

[3] J. Hauer, D. Trudnowski, and J. DeSteese, "A Perspective on WAMS Analysis Tools for Tracking of Oscillatory Dynamics," *IEEE PES General Meeting*, 2007.

[4] Y. Chompoobutrgool and L. Vanfretti, "On the Persistence of Dominant Inter-Area Oscillation Paths in Large-Scale Power Networks," 8^{th} *IFAC Symposium on Power Plants and Power Systems*, September 2-5 2012.

[5] ——, "Persistence of Multiple Interaction Paths for Individual Inter-Area Modes," 8^{th} *IFAC Symposium on Power Plants and Power Systems*, September 2-5 2012.

[6] L. Vanfretti, "Phasor Measurement-Based State Estimation of Electric Power Systems and Linearized Analysis of Power System Network Oscillations," Ph.D. dissertation, Rensselaer Polytechnic Institute, Troy, NY, USA, December 2009.

[7] L. Vanfretti and J. Chow, "Analysis of Power System Oscillations for Developing Synchrophasor Data Applications," *IREP Symposium - Bulk Power System Dynamics and Control*, 2010.

[8] R. Cresap and J. Hauer, "Emergence of a New Swing Mode in the Western Power System," *IEEE Transactions on Power Apparatus and Systems*, vol. PAS-100, no. 4, pp. 2037–2045, April 1981.

[9] J. H. Chow, G. E. Boukarim, and A. Murdoch, "Power System Stabilizers as Undergraduate Control Design Projects," *IEEE Transactions on Power Systems*, vol. 19, no. 1, pp. 144–151, February 2004.

[10] P. Kundur, *Power System Stability and Control*, N. J. Balu, Ed. McGraw-Hill, 1993.

[11] J. Chow and S. Ghiocel, *Control and Optimization Methods for Electric Smart Grids*. Springer Series in Power Electronics and Power Systems, 2012, ch. An Adaptive Wide-Area Power System Damping Controller using Synchrophasor Data.

[12] J. Chow, L. Beard, M. Patel, P. Quinn, A. Silverstein, D. Sobajic, and L. Vanfretti, "Guildelines for Siting Phasor Measurement Units," North American SynchroPhasor Initiative, Tech. Rep., June 2011. [Online]. Available: http://tinyurl.com/naspi-placement-guide